Trends in Sciences
TRENDS IN SCIENCES 2026; 23(2): 11122
DJMP Center for Digital Journal Management & Multidisciplinary Academic Platform
https://doi.org/10.48048/tis.2026.11122
RESEARCH ARTICLE

Unvealing the Electrokinetic Behavior of Nopal Mucilage Versus Polygalacturonic Acid for Multivalent Metal Interactions in Aqueous Systems

Eduardo Alberto López-Maldonado[1,*], Ana Isabel Ames Lopez[1],
Luis Miguel Lopéz-Martínez[2], José Manuel Cornejo-Bravo[1],
José Trinidad López-Maldonado[3], M. G. Romero-Sánchez[4] and J. M. Juarez-Lopez[5]

[1]Faculty of Chemical Sciences and Engineering, Autonomous University of Baja California, Mexicali B.C., Mexico
[2]Universidad Estatal de Sonora (UES), Sonora, México
[3]División de Tecnologías Industriales, Universidad Politécnica de Querétaro, Querétaro C. P., México
[4]Department Metal-Mecánica TecNM -Querétaro Santiago de Querétaro, Querétaro, México
[5]Agencia de Energía del Estado de Querétaro - Universidad Politécnica de Querétaro,
Santiago de Querétaro, Querétaro, México

([*]Corresponding author's e-mail: elopez92@uabc.edu.mx)

Received: 30 June 2025, Revised: 29 August 2025, Accepted: 5 September 2025, Published: 1 November 2025

Abstract

Natural polysaccharides have emerged as promising alternatives to synthetic polymers in wastewater treatment because of their functional versatility, environmental compatibility, and cost-effectiveness. In this study, mucilage extracted from *Opuntia ficus*-indica (MNE) and commercial polygalacturonic acid (PGA) were investigated for their structural and electrokinetic behavior during interactions with multivalent metal ions. The biopolymers were characterized by FTIR spectroscopy, which revealed fundamental differences in the functional group composition, mainly in terms of the esterification and ionization of the carboxyl groups. Zeta potential (ζ) measurements were performed over a pH range and under titration with selected metal ions (Ca^{2+}, Cr^{3+}, Cu^{2+}, Pb^{2+}, Zn^{2+}, Ni^{2+} and Cd^{2+}), which provided information on their dose–response and affinity profiles. MNE showed moderate surface charge variability and progressive shifts in ζ, implying heterogeneous binding interactions; PGA presented more abrupt and stronger electrostatic changes owing to its linear uniform structure. This study revealed that both substances could be good for removing heavy metals, which is important for the creation of eco-friendly clumping agents and sticky substances. This study aids in understanding how the form and purpose of these substances are related to naturally charged polymers and backs their use in eco-friendly purification methods.

Keywords: *Opuntia ficus*-indica, Nopal mucilage, Polygalacturonic acid, Zeta potential, Metal ion-polyelectrolyte interaction, Water treatment

Introduction

The Opuntia genus, and more specifically *Opuntia ficus*-indica, is known as one of the most bioavailable vegetables that produces mucilage, and mucilage is considered a complex heteropolysaccharide with extremely high water retention ability and is utilized as an industrial hydrocolloid of a sustainable nature [1-4]. The main sugar components of nopal mucilage are L-arabinose, D-galactose, L-rhamnose, D-xylose and galacturonic acid, but the quantity can vary, with a compositional range of arabinose (24.6% - 42%), galactose (21% - 40.1%), galacturonic acid (8% - 12.7%), rhamnose (7% - 13.1%) and xylose (22% - 22.2%) [5,6]. Its molecular weight, like that of other biopolymers, can range from 2.3×10^4 to 3×10^6 $g\cdot mol^{-1}$, under extraction procedures and purification degrees [5-8]. Historically, nopal mucilage has been studied for use as a food, cosmetic, and construction material in light of its thickening, emulsifying, and adhesive characteristics [6,9,10]. However, lately, more attention has been given to its environmental applications, particularly in water treatment systems. Owing to its natural characteristics, mucilage has carboxyl (COO) and hydroxyl (OH) groups, which enable it to interact with multivalent metal ions [11,12]; therefore, mucilage is a promising alternative low-cost, biodegradable biosorbent and coagulant reused in the wastewater treatment process [9,12]. Heavy metal contamination in aquatic environments remains a significant concern because of its persistence, bioaccumulation, and toxicity to living organisms [13]. In traditional technologies for eliminating metal ions from industrial wastewater, such as chemical precipitation, ion exchange, and membrane separation, the operation cost is typically high, the efficiency at low metal concentrations is low, and toxic sludge is produced; therefore, these methods are not widely applied [11,12,14]. Accordingly, it has become increasingly desirable to focus attention on biopolymer-based technologies that could offer cost-effective and environmentally friendly alternatives [11].

The use of natural coagulants for coagulation and flocculation has been increasingly developed in recent years [15]. These phenomena are regulated by theories such as DLVO, which describes the equilibrium between electrostatic repulsion forces and van der Waals attraction forces between colloidal particles. Colloid destabilization is fundamentally produced through the control of surface charge, which is commonly conducted via techniques such as pH adjustment, or through the introduction of charged (bio)polymers that are able to bridge or neutralize the suspended particles [16,17]. Natural organic polymers such as chitosan and tannin derivatives have been reported to be highly efficient biocoagulants, and their high efficiency has led to the search for other plant product substitutes [18,19]. Polygalacturonic acid (PGA), a homopolymer of α-1,4-linked D-galacturonic acid and major structural backbone of pectins, has been widely used as a model reference material to investigate the binding molecular mechanisms of metal ions [12]. Owing to its well-characterized structure and high concentration of COOH groups, PGA has been widely used for the adsorption, coordination, and colloidal stability of metal cations [20]. However, to our knowledge, very few studies have compared the metal binding capacity of PGA to that of complex plant mucilages such as those extracted from nopal.

In this work, we investigated the structural and electrokinetic properties of nopal mucilage extract (MNE) in comparison with those of commercial PGA, with the aim of understanding their potential as biobased materials for heavy metal interactions and removal. Through a combination of FTIR spectroscopy and zeta potential analysis, we evaluated the functional group composition, ionization behavior (pKa-related), and surface charge dynamics of both materials under various pH conditions. Additionally, we assess their affinity toward selected metal ions (Ca^{2+}, Cu^{2+}, Pb^{2+}, Cr^{3+}, Ni^{2+} and Zn^{2+}) via a systematic titration-based approach. This comparative study contributes novel insights into the physicochemical properties that govern the interactions of metal ions with natural polysaccharides and supports the development of sustainable materials for water purification applications.

Materials and methods

Extraction of nopal mucilage

Fresh cladodes of *Opuntia ficus*-indica were harvested from cultivated fields in Baja California, Mexico, and used as the raw material for mucilage extraction. After manual cleaning to remove external debris, the cladodes were diced into 2 cm cubes and blended with distilled water at a 1:2 (w/v) ratio using a household blender for 5 min to obtain a homogeneous slurry (**Figure 1**) [21]. The mixture was then thermally treated at 90 °C for 60 min under continuous stirring to facilitate the release of mucilaginous compounds. After cooling to room temperature, the suspension was filtered through a fine-mesh stainless steel sieve to remove insoluble plant residues [22].

The filtrate was subjected to centrifugation via a Beckman Coulter Eppendorf 5804R centrifuge at 5,000 rpm for 6 min. The resulting supernatant, containing the dissolved mucilage, was collected and subjected to precipitation by the addition of 96% ethanol at a 1:4 volume ratio. The system was gently stirred and allowed to rest, promoting mucilage aggregation. The precipitated solid was recovered by a second centrifugation step (5,000 rpm, 6 min), and the pellet was dried at 60 °C for 3 h in a convection oven. Finally, the dried mucilage was ground using a porcelain mortar and pestle to obtain a uniform fine powder. The final mucilage yield was approximately 0.25 %(w/w), calculated as grams of dry mucilage per 100 g of fresh cladode material (**Figure 1**).

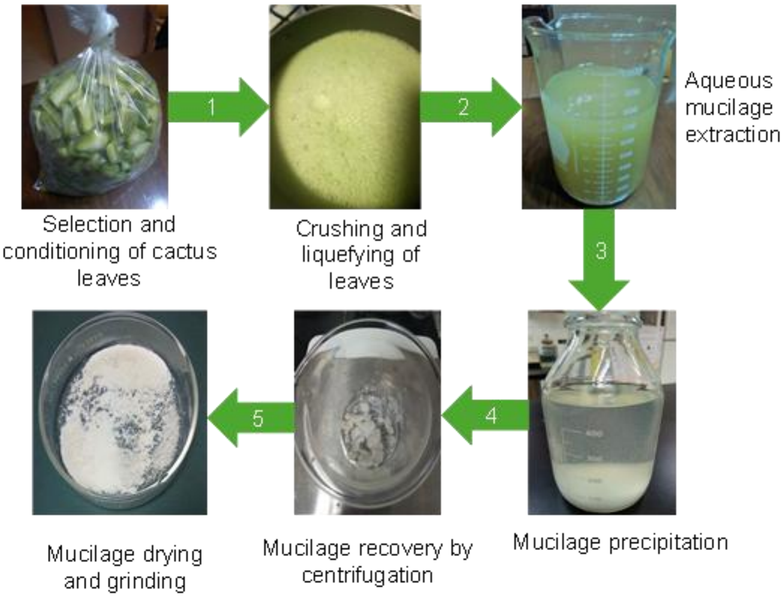

Figure 1 Mucilage extraction from cactus (*Opuntia ficus*-indica).

Physicochemical characterization of MNE

Fourier transform infrared spectroscopy (FTIR)

FTIR was used to identify the functional groups present in the extracted mucilage. Approximately 1 mg of dried MNE powder was analyzed via a Perkin-Elmer Spectrum 100 spectrometer (Perkin Elmer Cetus Instruments, Norwalk, CT, USA). The spectra were recorded in transmission mode in the range of 4,000 - 1,000 cm^{-1}, with a spectral resolution of 2 cm^{-1}, using KBr as a diluent.

The degree of methoxylation was calculated as follows [12]:

$$DM(\%) = \frac{A_{1740}}{A_{1740}+A_{1630}} \times 100 \tag{1}$$

where A_{1740} and A_{1630} are the corrected absorbance areas of the ester and carboxylate bands, respectively.

Zeta potential (ζ) profile as a function of pH

To assess the surface charge behavior of MNEs under various pH conditions, a 0.1% (w/w) aqueous solution was prepared in Milli-Q® water. The pH was adjusted stepwise to 3, 5, 7, 9, and 11 via incremental additions (10 µL every 20 s) of 0.1 M NaOH and 0.1 M HCl solutions. Zeta potential measurements were performed at each pH level via a Zetasizer Nano NS instrument (Model DTS 1060; Malvern Instruments, Miami, FL, USA) equipped with a 532 nm laser source and graphite electrodes [16]. Chitosan was used as a reference material to verify instrument performance and calibration.

Metal ion affinity testing

To evaluate the chemical affinity of MNEs for selected metal ions, aqueous solutions of analytical-grade salts - $Ca(NO_3)_2 \cdot 4H_2O$, $Cr(NO_3)_3 \cdot 9H_2O$, $Zn(NO_3)_2 \cdot 6H_2O$, $Ni(NO_3)_2$, $Cu(NO_3)_2$, and $Pb(NO_3)_2$ - were prepared at a fixed concentration of 0.1 M in Milli-Q® water. Metal ion addition experiments were conducted by adding 15 sequential aliquots of each metal mixture to 12 mL of 0.1 %(w/w) MNE solution. The total added metal concentrations ranged from 10 to 1,000 µmol per test, depending on the trial [19]. After each addition, the sample was stirred for 5 min at 60 rpm via a magnetic stirrer to ensure equilibrium. The pH was recorded via a Hach HQ40d multiparameter meter calibrated with standard buffer solutions. The conductivity and zeta potential were measured in triplicate for each condition via the same Zetasizer Nano NS instrument operating in autoaveraging mode (100 repetitions per measurement) to obtain reliable mean values [23].

Characterization of MNE before and after metal adsorption via X-ray photoelectron spectroscopy (XPS)

XPS was performed with a SPECS® spectrometer with a PHOIBOS® 150 WAL hemispherical energy analyzer with angular resolution (<0.5°) equipped with XR 50 X-ray and μ-FOCUS 500 X-ray monochromator (Al excitation line) sources.

Results and discussion

Spectroscopic and electrokinetic characterization of nopal biopolyelectrolyte: Insights from FTIR and zeta potential analysis

The chemical complexity and adsorption performance of natural polysaccharides are intimately related to their functional groups, molecular architecture, and charge density [12,23,24]. In this context, a comparative spectroscopic and structural analysis was conducted between MNE (**Figure 2**), commercial PGA, and the previously reported nopal pectin (NP) to elucidate their potential as biosorbents for heavy metal ions [12].

The FTIR spectra of MNE and PGA (**Figure 2(a)**) exhibit characteristic bands consistent with polysaccharidic structures but with distinct intensities and peak distributions reflecting differences in purity and polymer homogeneity [12]. The broad and intense absorption band near 3,400 cm^{-1} in both samples is assigned to O-H stretching vibrations, indicating the presence of abundant hydroxyl groups. Notably, this band is more pronounced in the MNE spectrum, suggesting a higher moisture affinity and a more disordered hydrogen-bonding network, typical of partially purified heteropolysaccharides (**Figure 2(a)**) [5,10].

A strong band at 1,735 cm^{-1}, assigned to esterified carboxyl groups (-COOCH$_3$), is evident in the PGA spectrum, but the band is either absent or very weak in the MNE spectrum [12,20]. MNE is inferred to be poorer in methoxylated residues because it is less processed and richer in free uronic acids [12]. The region of 1,600 - 1,400 cm^{-1} in both spectra is clearly the region of the asymmetric (1,605 cm^{-1}) and symmetric (~1,420 cm^{-1}) stretching vibrations of carboxylate anions (-COO$^-$) [3,25]. However, the intensity is much greater in PGA, which is indicative of its homogeneous component in galacturonic acid and high charge density [9,26]. The mucilage nopal extract presented a DM of approximately 84% on the basis of peak height analysis, indicating a highly esterified structure [6,12]. In contrast, commercial polygalacturonic acid exhibited an almost negligible ester band (DM ≈ 0%), whereas the nopal pectin reported in the literature presented a value near 65%. These findings are consistent with published FTIR data for NPs, which confirmed similar functional groups and a DM of approximately 65% [12]. This composition reflects the coexistence of esterified and ionized carboxyl groups, positioning the NP at an intermediate level of methoxylation between the highly esterified MNE and the de-esterified PGA [11,12].

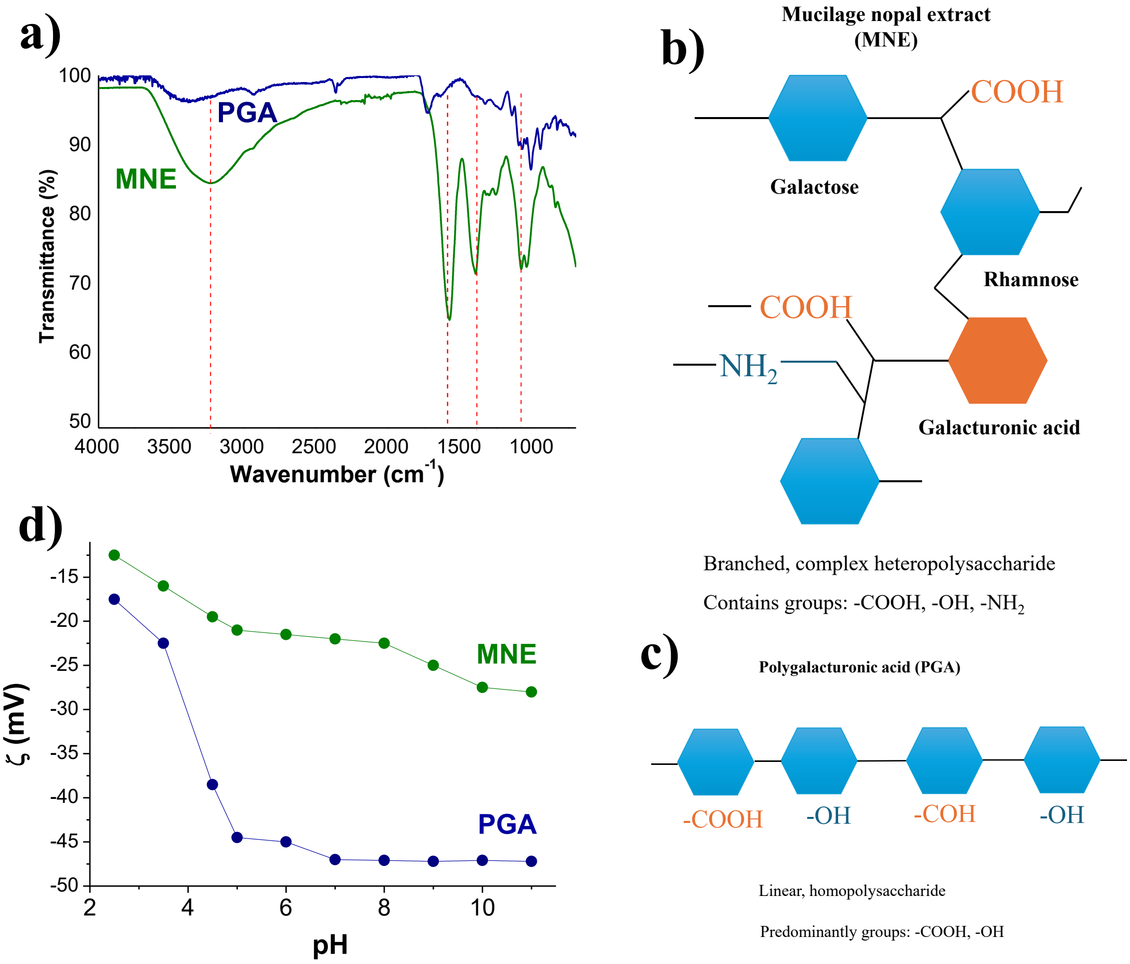

Figure 2 Structural and electrokinetic characterization of natural mucilage extract (MNE) and polygalacturonic acid (PGA): (a) Fourier transform infrared (FTIR) spectral comparison of MNE and PGA, illustrating key functional groups involved in metal coordination; (b) Proposed macromolecular model for the mucilage extracted from *Opuntia ficus*-indica (MNE), highlighting the heterogeneous polysaccharide backbone with potential metal-binding domains; (c) Proposed linear structure of PGA, composed predominantly of D-galacturonic acid residues enabling uniform ion complexation; (d) Zeta potential profiles of MNE and PGA as a function of pH, indicating surface charge behavior critical for colloidal destabilization.

MNE is a heterogeneous blend of neutral and acidic polysaccharides such as arabinose, rhamnose, galactose, and uronic acids (**Figure 2(b)**). The nonlinear structure and wide range of branching levels lowers the spectral resolution but may give rise to a variety of attachment sites via -OH and -COOH groups; additionally, it would enhance polyvalent ion attraction through myriad binding modes. In contrast, PGA is a linear homopolymer of α-(1→4)-linked D-galacturonic acid monomers with a high carboxyl group content and few side chains (**Figure 2(c)**) [27]. This structure provides uniform chelation behavior and uniform physicochemical properties and is an excellent model for mechanistic studies of metal coordination [12].

NP represents a semipurified intermediate, retaining the essential galacturonic backbone with partial esterification, as well as minor amounts of neutral sugars. Its DM (~65%) supports both electrostatic and coordination mechanisms for metal ion removal, which are modulated by the solution pH and ionic strength [12].

The results of the ζ measurements corroborate the FTIR findings. In **Figure 2(d),** PGA displays a consistently negative ζ value (approximately −40 mV) across a broad pH range (4 - 10), indicative of a high density of free carboxylate groups and a stable colloidal dispersion. In contrast, MNEs exhibit a lower ζ potential (–20 to –35 mV), with more pronounced variation across pH. This is attributed to its heterogeneity and the presence of protonatable groups, which modulate its surface charge and aggregation behavior [19].

The ζ profile reported for NP shows a weaker charge (ca. –4 mV) at neutral pH, which is consistent with its partial methoxylation. Despite the lower ζ magnitude, the NPs effectively removed more than 90% of the Cu^{2+}, Zn^{2+}, and Cr^{3+} under optimized conditions (pH 4 - 5) because of the combined action of electrostatic attraction and coordination with the carboxyl and hydroxyl groups [12,18].

The acid-base dissociation behavior of carboxylic groups plays a central role in determining the availability of binding sites for metal ions. The effective pKa values of galacturonic acid residues in these materials typically range from 3.4 - 4.2, depending on the degree of esterification and the local microenvironment. At pH < pKa, carboxylic groups remain protonated (-COOH), limiting their ability to chelate metal ions. Conversely, pH > pKa promotes ionization to the carboxylate form ($-COO^-$), increasing the negative surface charge and the electrostatic affinity for divalent and trivalent cations [19].

In the case of PGA, nearly complete de-esterification results in a sharp transition in charge behavior near its intrinsic pKa (3.5), leading to strong and consistent ionization at mildly acidic to neutral pH. This behavior is reflected in its highly negative ζ-potential values (–40 mV) from pH 4 - 10, indicating stable colloidal dispersion and surface charge uniformity.

For MNE, the situation is more complex. Given its heterogeneous composition, the effective pKa is distributed over a broader range, with overlapping contributions from uronic acids, neutral sugars, and residual proteins. Experimental zeta potential measurements (**Figure 2(c)**) reveal ζ values ranging from –20 to –35 mV depending on pH, confirming the presence of functional acidic groups but also indicating a less homogeneous ionization profile [19]. The onset of carboxylate formation at approximately pH 4 aligns with the dissociation of uronic acids, enabling greater metal affinity under slightly acidic conditions [28].

NP, with its partial methoxylation, has a less negative surface charge (ζ ≈ –4 mV); however, the presence of both COO^- and $COOCH_3$ groups offers versatile binding modes - electrostatic attraction from the carboxylates and potential cation - dipole interactions with esterified groups [12]. The DM (degree of methylation) modulates the pKa values of individual carboxyl groups: Methoxylated residues typically exhibit higher pKa values due to decreased polarity, thus ionizing only under alkaline conditions [12].

Zeta potential measurements assessing the interaction of metal ions (M^{n+}) with nopal mucilage extract and polygalacturonic acid

Figure 3 shows the zeta potential titration profiles for MNE and PGA at a 0.1% (w/w) concentration after incremental additions of selected divalent and trivalent metal ions (Cr^{3+}, Cu^{2+}, Pb^{2+}, Zn^{2+}, Ni^{2+}, Cd^{2+} and Ca^{2+}). The behavior observed in both systems reflects distinct interaction mechanisms that are strongly influenced by the polymer composition, functional group availability, and structural conformation.

In the case of MNE (**Figure 3(a)**), the initial zeta potential at 0 metal addition is moderately negative (approximately –25 to –30 mV), indicating the presence of ionizable acidic groups, primarily carboxyl and hydroxyl moieties derived from uronic acids and neutral sugars. Upon progressive metal addition, a gradual reduction in the negative surface charge is observed for all the cations tested, with the rate and extent of neutralization varying by metal type. Notably, trivalent Cr^{3+} and divalent Pb^{2+} induce the most pronounced shifts toward neutral or slightly positive ζ values, suggesting a strong affinity for surface binding sites, likely due to their higher charge density and smaller hydrated ionic ratio [13]. The steeper decrease in ζ with these ions may also reflect the onset of bridging or crosslinking interactions between adjacent mucilage chains [24].

Conversely, the addition of Zn^{2+}, Ni^{2+}, and Cd^{2+} results in more moderate shifts, possibly due to weaker electrostatic interactions or limited coordination geometry with the available ligands on the polymer matrix. The response to Ca^{2+} is particularly relevant, as it represents a physiological divalent ion commonly used to probe crosslinking in pectic and mucilaginous materials. The consistent trend across Ca^{2+} and the other metals confirms the polyanionic nature of MNE and its potential for polyvalent cation sorption.

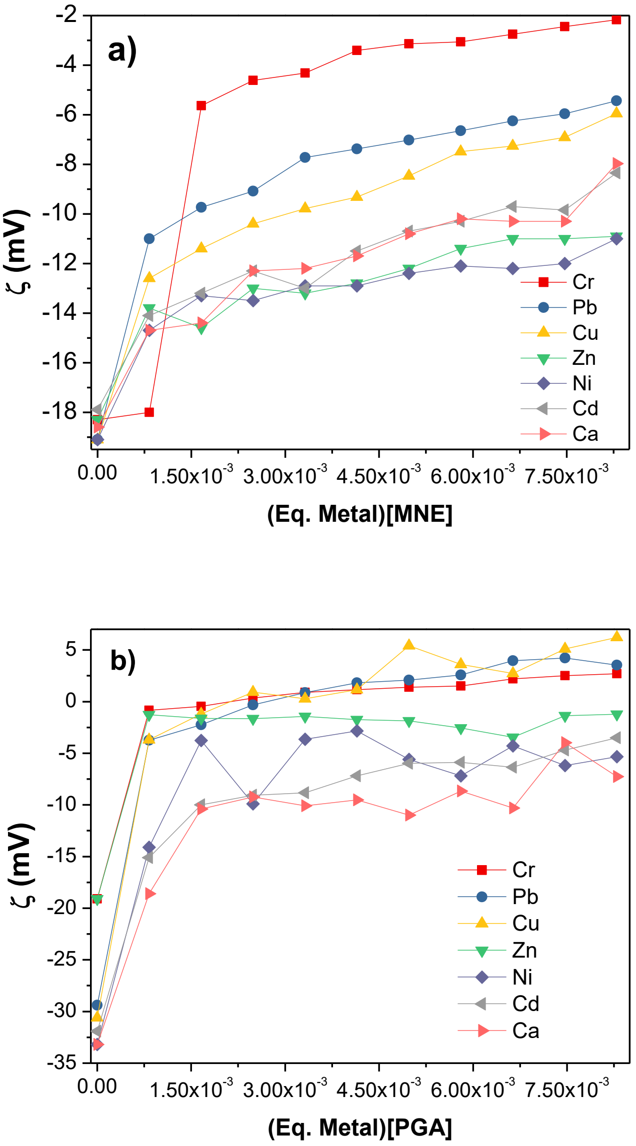

Figure 3 Titration profiles of (a) nopal (*Opuntia* spp.*)* mucilage (MNE) (0.1%, p/p), and (b) galacturonic acid (PGA) (0.1%, p/p) with different metals (Cr^{3+}, Cu^{2+}, Pb^{2+}, Zn^{2+}, Ni^{2+}, Cd^{2+} and Ca^{2+}) by zeta potential.

For PGA (**Figure 3(b)**), the initial zeta potential is significantly more negative (approximately –40 mV), which is consistent with its composition as a homopolymer of galacturonic acid with a high density of deprotonated carboxyl groups at neutral pH. The titration curves reveal sharper transitions with metal addition than with MNE, particularly for Cr^{3+} and Cu^{2+}, suggesting more uniform and efficient electrostatic interactions. This behavior reflects the structural simplicity and greater charge regularity of PGA, which facilitates a predictable collapse of the surface charge upon cation complexation.

Interestingly, although PGA and MNE share common functional groups ($–COO^-$), their interaction profiles diverge owing to differences in molecular architecture. MNE, a heteropolysaccharide with branched chains and residual neutral sugars, may exhibit steric hindrance and less efficient ion coordination per unit mass. In comparison, PGA presents linear and largely accessible binding sites, thus promoting cooperative binding and more rapid changes in the zeta potential. PGA is a good polyelectrolyte model for adsorption studies because of its ability to have near-neutral or positive ζ-values for relatively low metal concentrations [11].

These results highlight the importance of both structural homogeneity and functional group density in determining the electrokinetic behavior of biopolymers upon interaction with a metal. MNE has chemical diversity and potential for multiple functions, whereas PGA is less chemically diverse and more explicit and controlled in terms of its behavior, which is beneficial for understanding its mechanism. The variation among the metals studied is also noteworthy and confirms the selective nature of these materials (able to be controlled according to pH, ionic strength or the derivatization of the polymer), which might be tailored in future applications [18].

Association constants (K_a) for MNE and PGA

The zeta potential changes linearly as the metal concentration increases with respect to the polymer concentration, $[M]_t/[L]_t$, suggesting the formation of complexes. By changing the present zeta potential, the formation constant (*K*) was calculated via a nonlinear model reported by Thordarson [29] as follows:

$$\zeta_{obs} = \zeta_H + 0.5\Delta\zeta_{\infty}\left\{\frac{[H]_T + [G]_T + \frac{1}{K} - \sqrt{\left([H]_T + [G]_T + \frac{1}{K}\right)^2 - 4[H]_T \times [G]_T}}{[H]_T}\right\} \quad (2)$$

where ζ_{obs} is the observed zeta potential, ζ_H is the zeta potential of the free polymer, $\Delta\,\zeta_{\infty}$ is the maximum zeta potential change induced by the presence of a given guest, $[G]_T$ is the total concentration of the guest, $[H]_T$ is the total concentration of the polymer, and K is the association constant. **Table 1** lists the association constants (K_a) for the complex, which ranged from approximately 10^2 - 10^4.

Table 1 Association constants (K_a) for MNE and PGA toward different metal ions.

Compound	**Metal**						
	Cr^{3+}	**Cu^{2+}**	**Pb^{2+}**	**Zn^{2+}**	**Ni^{2+}**	**Cd^{2+}**	**Ca^{2+}**
	K_a	K_a	K_a	K_a	K_a	K_a	K_a
MNE	6.944×10^2 M^{-1}	9.345×10^2 M^{-1}	1.871×10^3 M^{-1}	8.772×10^2 M^{-1}	2.132×10^3 M^{-1}	4.464×10^2 M^{-1}	4.424×10^2 M^{-1}
PGA	1.346×10^4 M^{-1}	5.801×10^3 M^{-1}	6.190×10^3 M^{-1}	ND	6.127×10^3 M^{-1}	2.674×10^3 M^{-1}	3.000×10^3 M^{-1}

ND: Not determined due to high affinity.

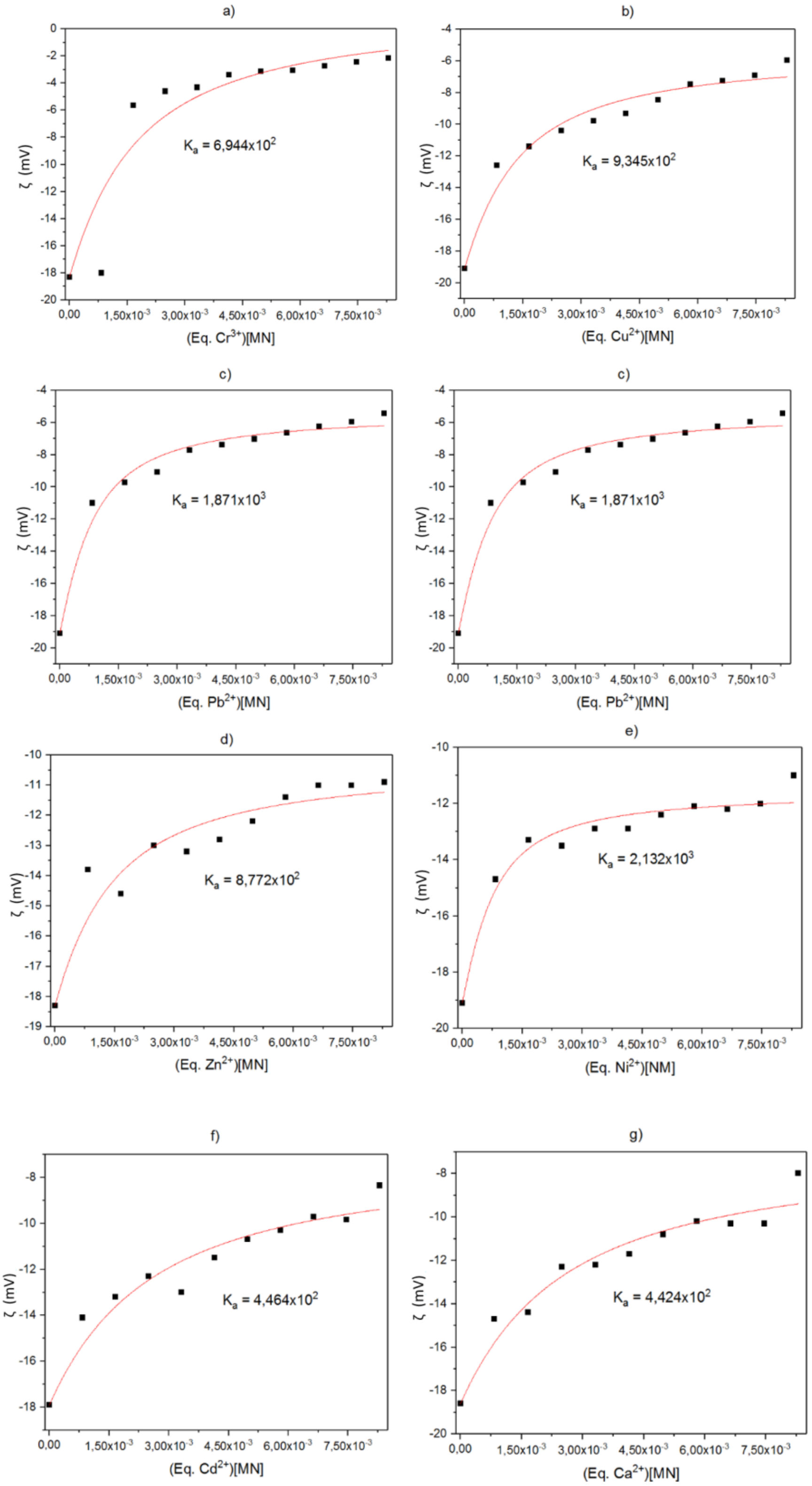

Figure 4 Association constants (K_a) for nopal (*Opuntia* spp.*)* mucilage toward different metal ions: (a) Cr^{3+}, (b) Cu^{2+}, (c) Pb^{2+}, (d) Zn^{2+}, (e) Ni^{2+}, (f) Cd^{2+} and (g) Ca^{2+}.

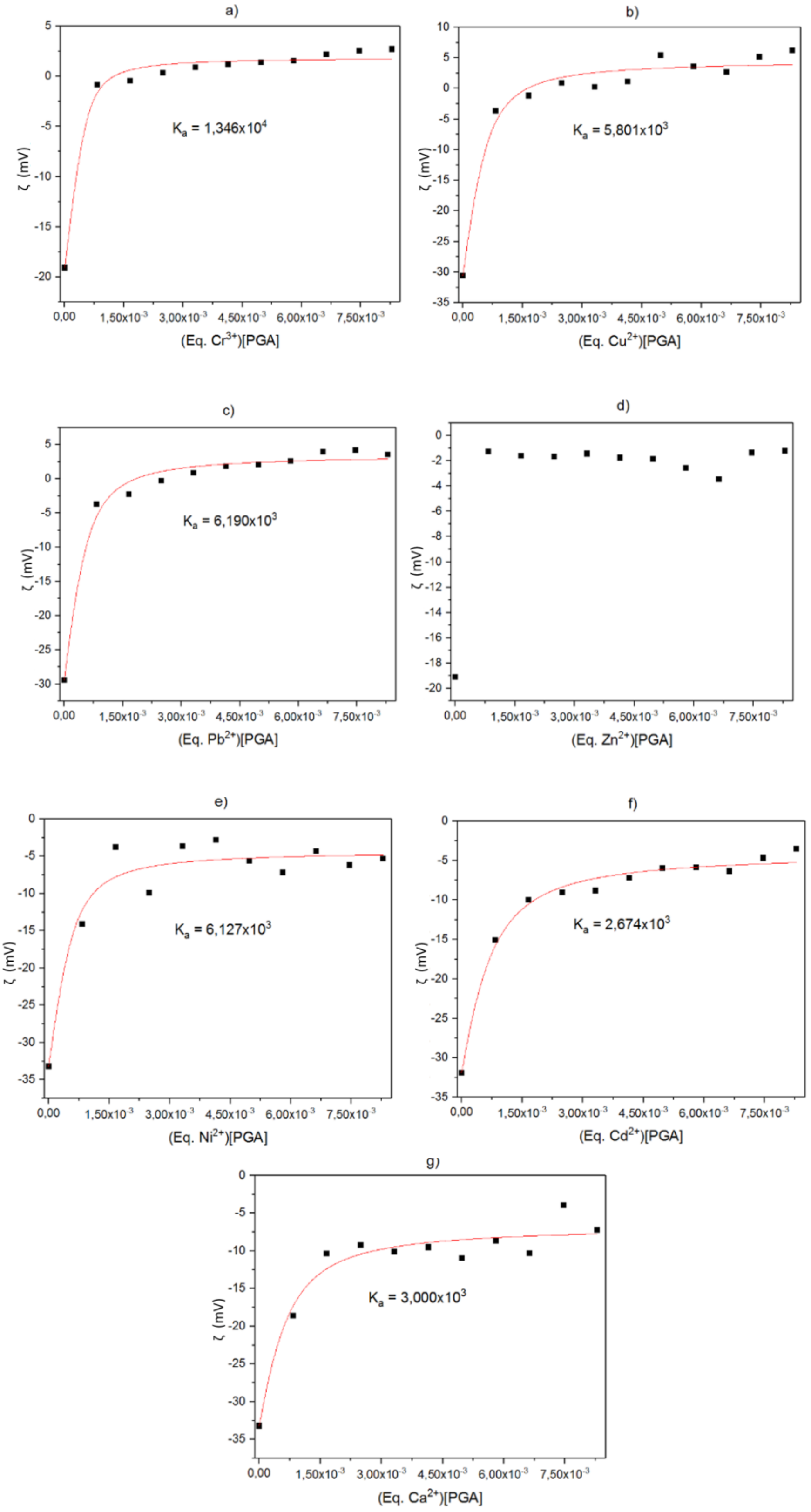

Figure 5 Association constants (K_a) for galacturonic acid (PGA) with different metal ions: (a) Cr^{3+}, (b) Cu^{2+}, (c) Pb^{2+}, (d) Zn^{2+}, (e) Ni^{2+}, (f) Cd^{2+} and (g) Ca^{2+}.

Figures 4 and **5** illustrate the association constants derived from the interactions of selected metal ions with MNE and PGA, respectively. These constants provide a quantitative measure of the binding strength between the biopolymers and the metals, offering a complementary perspective to the zeta potential analysis discussed previously.

For MNE, the trend in metal affinity follows the order: $Cu^{2+} > Zn^{2+} > Cr^{3+} > Cd^{2+} > Ca^{2+} > Ni^{2+} > Pb^{2+}$. This hierarchy suggests that MNEs exhibit a greater binding preference for transition metals with intermediate charge density and moderate ionic radii, such as Cu^{2+} and Zn^{2+} (**Figure 4**). The relatively strong interaction with Cr^{3+}, despite its higher valency, may be attributed to specific coordination with oxygen-containing groups, although steric hindrance and structural disorder in the mucilage matrix might limit more efficient complex formation with other trivalent ions. The lower Ka values observed for Ni^{2+} and Pb^{2+} could reflect either reduced compatibility with available binding sites or less favorable hydration energies during coordination [13].

In contrast, PGA exhibited markedly different interaction profiles, with the following order of binding strength: $Zn^{2+} > Pb^{2+} > Ni^{2+} > Cu^{2+} > Ca^{2+} > Cd^{2+} > Cr^{3+}$ (**Figure 5**). The preferential affinity toward Zn^{2+} and Pb^{2+} suggests that the uniform linear structure and dense array of deprotonated carboxylate groups of PGA facilitate more stable electrostatic and chelating interactions, particularly with metals that exhibit borderline Lewis acid character [30]. Interestingly, Cr^{3+} - a strong Lewis acid - displays the weakest interaction with PGA among all the tested ions, potentially due to steric constraints in the formation of inner-sphere complexes along the tightly packed polymer backbone [19,31]. This behavior contrasts with its stronger interaction in MNE, underscoring the role of polymer architecture and flexibility in modulating metal coordination.

The divergence in metal-binding patterns between MNE and PGA reinforces the importance of structural heterogeneity in defining sorption selectivity. MNE, which is rich in neutral sugars and features a branched conformation, provides a wider range of microenvironments and binding motifs that may favor diverse and dynamic interactions, albeit with less predictability. In contrast, PGA continues to respond consistently because of its chemically uniform and sterically accessible structure, which is ideal for site specific, reproducible binding, especially in applications requiring an ordered metal withdrawal mechanism.

These results suggest that MNEs may provide a more general, polyvalent binding ability that is appropriate for complex wastewater matrices and that PGA is a suitable model for systems that require specific ion capture behavior. Overall, combined applications of the 2 materials in a composite or a hybrid system may be interesting for improving the flexibility and efficiency of biopolymer-based methods used for the removal of metal ions from an aqueous medium.

X-ray photoelectron spectroscopy (XPS) of the MNE before and after adsorption of metal ions

XPS analysis revealed substantial changes in the surface composition of the cactus mucilage before and after the adsorption of heavy metals. In the initial sample, the high-resolution C1 s and O1 s spectra displayed characteristic peaks assigned to C-C/C-H (~284.8 eV), C-O (~286.4 eV), and C=O (~288.0 eV), confirming the predominance of polysaccharides and carboxylic groups typical of pectin and other polysaccharide fractions [32]. The O1 s signal (~531 - 533 eV) was dominated by oxygen in the C-O and C=O bonds, with an O/C ratio consistent with that of polysaccharide-based biopolymers. After adsorption, new signals and shifts in the main peaks were observed. Notably, components attributable to metallic species emerged (e.g., characteristic peaks of Pb 4f, Cd 3d, or Cu 2p, depending on the metals present in the system), confirming the surface fixation of metal ions [30]. Furthermore, the binding energy shifts in C1s and O1s suggest the formation of coordinated interactions between the mucilage's carboxylate/hydroxyl groups and the metal cations, a phenomenon widely reported in biopolymers with complexation capacity. These results not only confirm the effectiveness of cactus mucilage as a bioadsorbent but also provide mechanistic evidence at the surface level, suggesting that its structure, which is rich in pectins and hemicelluloses, is key for interactions with multivalent cations [33]. The observed behavior is consistent with previous studies on plant-based biopolymers but is particularly noteworthy because of the use of a nonconventional, low-cost biomass with high availability in arid regions.

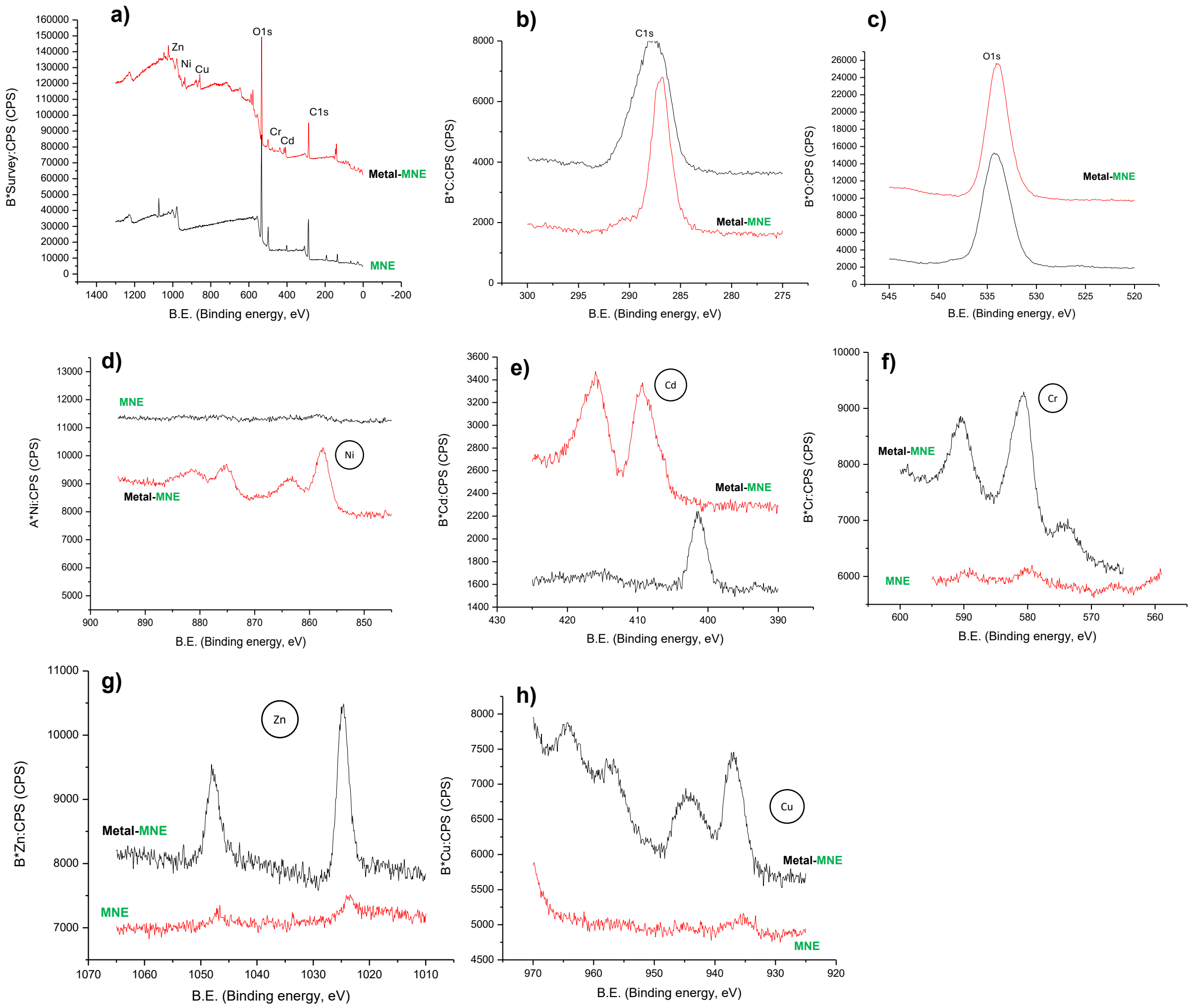

Figure 6 XPS general survey of the MNE before and after adsorption of metal ions.

Mechanistic and application-oriented insights into MNE and PGA for metal removal

The molecular interactions observed for MNE and PGA also reveal their practical importance in water purification [34]. Their distinctive electrokinetic responses and structural features provide valuable guidance for optimizing coagulation, flocculation, and sedimentation processes, contributing to more effective strategies in environmental remediation (**Table 2**).

MNE presents a structurally diverse matrix consisting of monosaccharides, including arabinose, rhamnose, galactose, xylose, and galacturonic acid. This intricacy allows for various binding mechanisms (**Figure 7**):

- Electrostatic attraction between deprotonated carboxyl groups (-COO$^-$) and metal cations;
- Hydrogen bonding involving hydroxyl groups and coordinated water molecules;
- Chelation through adjacent hydroxyl and carboxyl groups;
- Ion bridging, particularly with trivalent metals such as Cr^{3+}, promotes crosslinking and network stabilization.

PGA, a linear polymer made solely of D-galacturonic acid, has a more consistent binding profile that is governed primarily by electrostatic attraction and chelation. It promotes effective site-specific complexation, particularly with divalent ions such as Pb^{2+} and Zn^{2+} [3,19,22].

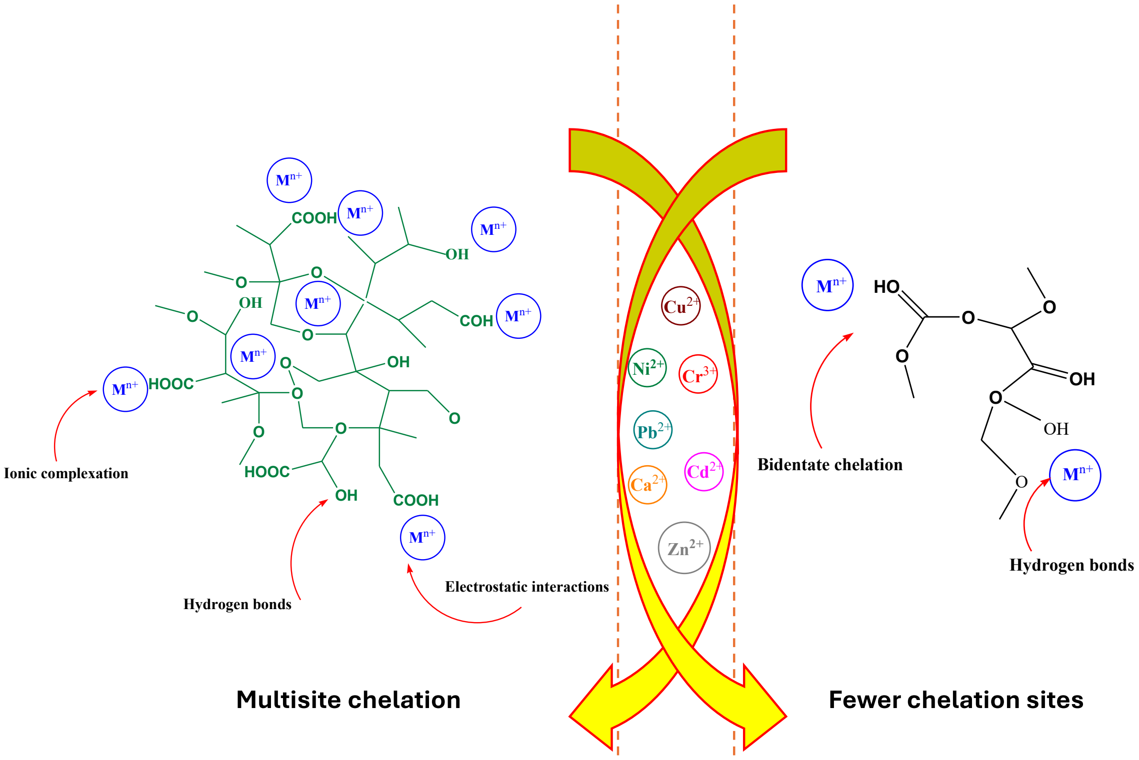

Figure 7 Mechanism of MNE and PGA for metal removal.

Comparative analysis of biopolyelectrolytes for electrokinetic applications in water treatment

Table 2 shows clear differences among the selected biopolyelectrolytes in terms of charge, functionality, and interaction pathways with metals. The MNE shows moderately negative potentials and dual -COOH/-OH groups, favoring binding through bridging and hydrogen bonds. PGA, with stronger negative values, acts mainly through chelation and charge neutralization. Alginate and pectin share comparable surface charges but differ in selectivity, which is influenced by the structural arrangement and density of their carboxyl groups [18]. Chitosan, which is positively charged under acidic conditions, interacts by inverting charge and bridging, resulting in an affinity for specific cations and oxyanions [35]. Taken together, these comparisons place the MNE in an intermediate position, combining features of both PGA and pectin, and underline its potential for multifunctional roles in water treatment. Although regeneration experiments were not part of the present work, previous reports indicate that plant-based polysaccharides are biodegradable and generally exhibit low toxicity, reinforcing their suitability for sustainable water treatment [33]. Their structural composition, dominated by hydroxyl and carboxyl groups, suggests that regeneration after metal adsorption could be achieved through mild treatments without major degradation of the polymer. These properties are particularly relevant for practical applications, where reusability and ecological safety are key requirements [11]. Future work will therefore prioritize evaluating regeneration performance and testing potential functional modifications to enhance the long-term applicability of MNE and PGA [34]. Although a fixed concentration was applied in this study, variations in polymer loading are known to alter charge neutralization and flocculation strength. Testing a broader range will be necessary to identify optimal conditions and translate these findings into practical treatment scenarios [16,18].

Table 2 Electrokinetic properties and water treatment potential of select biopolyelectrolytes.

Polyelectrolytes	**Zeta Potential (mV)**	**Primary functional groups**	**Metal affinity**	**Predominant mechanism**	**Reference**
MNE (Opuntia mucilage)	–20 to –35	-COOH, -OH	$Cu^{2+} > Zn^{2+} > Cr^{3+}$	Polymeric bridging, H-bonding	This work
Polygalacturonic Acid	~–40	-COOH	$Zn^{2+} > Pb^{2+} > Cu^{2+}$	Charge neutralization, Chelation	This work
Alginate	–35 to –50	-COOH, -OH	$Pb^{2+} > Cd^{2+} > Ni^{2+}$	Ionic crosslinking	[18]
Chitosan	+10 to +35 (acidic pH)	$-NH_2$	$Cr^{6+} > As^{3+} > Cu^{2+}$	Charge inversion, Bridging	[20,36]
Pectin	–25 to –45	-COOH	$Pb^{2+} > Zn^{2+} > Cd^{2+}$	Chelation, Neutralization	[20,37]

Conclusions

This work provides new knowledge about the structural and electrokinetic properties of *Opuntia ficus*-indica mucilage compared with those of commercial polygalacturonic acid, especially in the context of their interaction with multivalent metal cations in aqueous media. The results of the FTIR study confirmed the major differences in the levels of esterification and the number of ionizable groups, revealing that, compared with MNE, PGA presented a smoother, more carboxyl-enriched profile. This contributed to interesting differences in their zeta potential responses, where MNE presented more progressive and broad surface charge transitions, whereas PGA presented sharper and better defined responses in the presence of metals.

Zeta potential experiments via titration revealed metal-specific interaction patterns, with Cr^{3+} and Pb^{2+} leading to the highest zeta potential neutralization in both biopolymers. These results were reinforced by the calculated association constants (Ka, 10^2 - 10^4 M^{-1}), demonstrating the affinity and selectivity of these biopolymers for specific cations. Notably, the MNE demonstrated diverse yet effective binding behavior, underscoring its potential as a sustainable, multifunctional material for the removal of heavy metals in water treatment systems.

In summary, while the PGA offers a controlled model system for mechanistic understanding, the MNE stands out for its ecological relevance, availability, and versatility. The comparative approach adopted here contributes to a deeper understanding of how the molecular structure and functional group composition influence the performance of natural PEs and opens pathways for the development of green technologies in environmental remediation.

Acknowledgements

The authors sincerely acknowledge the support provided by the participating institutions throughout the development of this research. Financial assistance from the Consejo Nacional de Humanidades, Ciencias y Tecnologías (CONAHCyT) under Grant No. A1-S-38139 is gratefully recognized. The authors thank the UABC for the funding granted to carry out this work with the internal project 300/4177.

Declaration of Generative AI in Scientific Writing

Not applicable.

CRediT Author Statement

Eduardo Alberto López-Maldonado: Conceptualization; Writing - Original Draft; Methodology; Writing - Review & Editing; Formal analysis; Validation; Project administration; Supervision; Software; Funding acquisition. **Ana Isabel Ames Lopez**: Investigation; Data curation; Formal analysis; Writing - Original draft preparation. **Luis Miguel Lopéz-Martínez**: Data curation; Visualization; Investigation. **José Manuel Cornejo-Bravo**: Visualization; Investigation. **José Trinidad López-Maldonado**: Software; Validation, Data Curation, Investigation. **M.G. Romero-Sánchez**: Formal analysis; Validation, Review & Editing. **J.M Juarez-Lopez:** Software, Visualization, Data curation.

References

[1] Y Choque-Quispe, AM Solano-Reynoso, D Choque-Quispe, CA Ligarda-Samanez, BS Ramos-Pacheco, Y Flores-Ccorisapra and YF Carhuarupay-Molleda. Optimization of the flocculating capacity of a new microatomization extract from a Nostoc cyanobacterium species from the High Andes. *Chemical Engineering Journal Advances* 2025; **23**, 100777.

[2] R Kamel, SM Afifi, IAA Kassem, NA Elkasabgy and MA Farag. Arabinoxylan and rhamnogalacturonan mucilage: Outgoing and potential trends of pharmaceutical, environmental, and medicinal merits. *International Journal of Biological Macromolecules* 2020; **165**, 2550-2564.

[3] N Sultana. Biological properties and biomedical applications of pectin and pectin-based composites: A review. *Molecules* 2023; **28(24)**, 7974.

[4] M Pierdomenico, P Giardullo, G Bruno, L Bacchetta, O Maccioni, OC Demurtas, M Sulli, C Arcangeli, F Colini, S Chiavarini and B Benassi. The mucilage from the *Opuntia ficus-indica* (L.) Mill. cladodes plays an anti-inflammatory role in the lps-stimulated HepG2 cells: A combined *in vitro* and *in silico* approach. *Molecular Nutrition & Food Research* 2025; **69(3)**, e202400479.

[5] S Trachtenberg and AM Mayer. Composition and properties of *Opuntia ficus-indica* mucilage. *Phytochemistry* 1981; **20(12)**, 2665-2668.

[6] C Sáenz, E Sepúlveda and B Matsuhiro. *Opuntia spp* mucilage's: A functional component with industrial perspectives. *Journal of Arid Environments* 2004; **57(3)**, 275-290.

[7] L Medina-Torres, ELF Brito-De, B Torrestiana-Sanchez and R Katthain. Rheological properties of the mucilage gum (*Opuntia ficus* indica). *Food Hydrocolloids* 2000; **14(5)**, 417-424.

[8] E Sepúlveda, C Sáenz, E Aliaga and C Aceituno. Extraction and characterization of mucilage in *Opuntia spp*. *Journal of Arid Environments* 2007; **68(4)**, 534-545.

[9] LMDC Coelho, BF Veloso, VDL Silva, LS Assunção, CDF Ribeiro and DM Otero. Innovations and challenges in the use of cactus mucilage: A technological analysis. *International Journal of Biological Macromolecules* 2025; **316**, 144792.

[10] AL García, CMP Zamora, AG Michaluk, MB Nuñez, AM González and CA Torres. Physicochemical and functional characterization of the mucilage obtained from cladodes of 2ss Opuntia species. *International Journal of Biological Macromolecules* 2024; **283**, 137802.

[11] EA López-Maldonado, Y Abdellaoui, MHA Elella, HM Abdallah, M Pandey, ET Anthony, L Ghimici, S Álvarez-Torrellas, V Pinos-Vélez and NA Oladoja. Innovative biopolyelectrolytes-based technologies for wastewater treatment. *International Journal of Biological Macromolecules* 2024; **273(2)**, 132895.

[12] D Ibarra-Rodríguez, J Lizardi-Mendoza, EA López-Maldonado and MT Oropeza-Guzmán. Capacity of 'nopal' pectin as a dual coagulant-flocculant agent for heavy metals removal. *Chemical Engineering Journal* 2017; **323**, 19-28.

[13] LEA López-Maldonado, H Hernández-García, MAM Zamudio-Aguilar, MT Oropeza-Guzmán, A Ochoa-Terán, LM López-Martínez, M Martinez-Quiroz, R Valdez and A Olivas. Chemical issues of coffee and Tule lignins as ecofriendly materials for the effective removal of hazardous metal ions contained in metal finishing wastewater. *Chemical Engineering Journal* 2020; **397**, 125384.

[14] EA López-Maldonado and MT Oropeza-Guzmán. Nejayote biopolyelectrolytes multifunctionality (glucurono ferulauted arabinoxylans) in the separation of hazardous metal ions from industrial wastewater. *Chemical Engineering Journal* 2021; **423**, 130210.

[15] A Martínez-Cruz, MNR Valencia, JA Araiza-Aguilar, HA Nájera-Aguilar and RF Gutiérrez-Hernández. Leachate treatment: Comparison of a biocoagulant (*Opuntia ficus* mucilage) and conventional coagulants using multicriteria decision analysis. *Heliyon* 2021; **7(7)**, e07510.

[16] EA López-Maldonado, MT Oropeza-Guzman, JL Jurado-Baizaval and A Ochoa-Terãn. Coagulation-flocculation mechanisms in wastewater treatment plants through zeta potential measurements. *Journal of Hazardous Materials* 2014; **279**, 1-10.

[17] H Alkhaldi, S Alharthi, S Alharthi, HA AlGhamdi, YM AlZahrani, SA Mahmoud, LG Amin, NH Al-Shaalan, WE Boraie, MS Attia, SA Al-Gahtany, N Aldaleeli, MM Ghobashy, AI Sharshir, M Madani, R Darwesh and SF Abaza. Sustainable polymeric adsorbents for adsorption-based water remediation and pathogen deactivation: A review. *RSC Advances* 2024; **14**, 33143-33190.

[18] EA López-Maldonado, OGZ García, KC Escobedo and MT Oropeza-Guzman. Evaluation of the chelating performance of biopolyelectrolyte green complexes (NIBPEGCs) for wastewater treatment from the metal finishing industry. *Journal of Hazardous Materials* 2017; **335**, 18-27.

[19] OGZ García, MT Oropeza-Guzmán, WMA Monal and EA López-Maldonado. Design and mechanism of action of multifunctional BPE's with high performance in the separation of hazardous metal ions from polluted water Part I: Chitosan-poly(N-vinylcaprolactam) and its derivatives. *Chemical Engineering Journal* 2019; **359**, 840-851.

[20] R Wang, R Liang, T Dai, J Chen, X Shuai and C Liu. Pectin-based adsorbents for heavy metal ions: A review. *Trends in Food Science & Technology* 2019; **91**, 319-329.

[21] M Quintero-García, E Gutiérrez-Cortez, M Bah, A Rojas-Molina, MA Cornejo-Villegas, AD Real and I Rojas-Molina. Comparative analysis of the chemical composition and physicochemical properties of the mucilage extracted from fresh and dehydrated *Opuntia ficus* indica cladodes. *Foods* 2021; **10(9)**, 2137.

[22] S Javed, Z Zulfiqar, Z Fatima, G Muhammad, MA Hussain, M Mushtaq and MT Haseeb. A comprehensive review of plant-based mucilages as promising candidates for water remediation. *Journal of Environmental Chemical Engineering* 2024; **12(5)**, 114035.

[23] CU Montaño-Medina, LM Lopéz-Martínez, A Ochoa-Terán, EA López-Maldonado, MI Salazar-Gastelum, B Trujillo-Navarrete, S Pérez-Sicairos and JM Cornejo-Bravo. New pyridyl and aniline-functionalized carbamoylcarboxylic acids for removal of metal ions from water by coagulation-flocculation process. *Chemical Engineering Journal* 2023; **451**, 138396.

[24] C Negro, WD Guerra, D Armentano, J Ferrando-Soria, T Grancha and E Pardo. Bioinspired metal-organic frameworks for aqueous environment decontamination: from laboratory scale to real-world technologies. *Chemical Communications* 2024; **60(100)**, 14935-14951.

[25] KM Wani and RVS Uppaluri. Characterization of pectin extracted from pomelo peel using pulsed ultrasound assisted extraction and acidic hot water extraction process. *Applied Food Research* 2023; **3(2)**, 100345.

[26] LS Brenda, GCG Martinez-Avila, H Rodriguez-Fuentes, LM Pastrana, AG Azevedo, DC González-Sandoval, MA Cerqueira and R Rojas. Extraction and characterization of mucilage from *Opuntia ficus*-indica cultivated on hydroponic system. *Notulae Botanicae Horti Agrobotanici Cluj-Napoca* 2022; **50(1)**, 12460.

[27] FM León-Martínez, PFJ Cano-Barrita, F Castellanos, KB Luna-Vicente, S Ramírez-Arellanes and C Gómez-Yáñez. Carbonation of high-calcium lime mortars containing cactus mucilage as additive: A spectroscopic approach. *Journal of Materials Science* 2021; **56(5)**, 3778-3789.

[28] I Donati and BE Christensen. Alginate-metal cation interactions: Macromolecular approach. *Carbohydrate Polymers* 2023; **321**, 121280.

[29] P Thordarson. Determining association constants from titration experiments in supramolecular chemistry. *Chemical Society Reviews* 2011; **40**, 1305-1323.

[30] R Liang, Y Li, L Huang, X Wang, X Hu, C Liu, M Chen and J Chen. Pb^{2+} adsorption by ethylenediamine-modified pectins and their

adsorption mechanisms. *Carbohydrate Polymers* 2020; **234**, 115911.

[31] S Deiana, L Erre, G Micera, P Piu and C Gessa. Coordination of transition-metal ions by polygalacturonic acid: A spectroscopic study. *Inorganica Chimica Acta* 1980; **46**, 249-253.

[32] X Yang, B Feng, Z Wang, L Jiang and J Bayoundoula. Aggregation relations and flotation behavior of the depressant pectin on talc, chlorite, and serpentine and its mechanism of action. *Minerals Engineering* 2025; **233**, 109637.

[33] HE Al-Hazmi, J Łuczak, S Habibzadeh, MS Hasanin, A Mohammadi, A Esmaeili, SJ Kim, MK Yazdi, N Rabiee, M Badawi and MR Saeb. Polysaccharide nanocomposites in wastewater treatment: A review. *Chemosphere* 2024; **347**, 140578.

[34] EA López-Maldonado, M Mavaei, S Dan, SN Banitaba, M Gholamhosseinpour, S Hamedi, LJ Villarreal-Gómez, GL Pérez-González, S Mashkouri, S Khademolqorani and AM Elgarahy. Diverse applications of versatile quaternized chitosan salts: A review. *International Journal of Biological Macromolecules* 2024; **281**, 136276.

[35] OGZ García, MT Oropeza-Guzmán, WMA Monal and EA López-Maldonado. Design and mechanism of action of multifunctional BPE's with high performance in the separation of hazardous metal ions from polluted water Part I: Chitosan-poly(N-vinylcaprolactam) and its derivatives. *Chemical Engineering Journal* 2019; **359**, 840-851.

[36] R Yang, H Li, M Huang, H Yang and A Li. A review on chitosan-based flocculants and their applications in water treatment. *Water Research* 2016; **95**, 59-89.

[37] H Salehizadeh, N Yan and R Farnood. Recent advances in polysaccharide biobased flocculants. *Biotechnology Advances* 2018; **36(1)**, 92-119.